Heliyon 11 (2025) e41897

Contents lists available at ScienceDirect

Heliyon

journal homepage: www.cell.com/heliyon

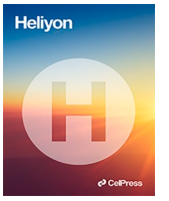

Research article

Identification of natural phytochemicals as AKT2 inhibitors using molecular docking and dynamics simulations as potential cancer therapeutics

Jibon Kumar Paul, Mahir Azmal, Md Naimul Haque Shohan, Mohua Mrinmoy, ANM Shah Newaz Been Haque, Omar Faruk Talukder, Ajit Ghosh *

Department of Biochemistry and Molecular Biology, Shahjalal University of Science and Technology, Sylhet, 3114, Bangladesh

ARTICLE INFO

Keywords:
ATK2
Molecular docking
Molecular dynamics simulation
Uzarigenin
Oncogenesis

ABSTRACT

The PI3K/AKT/mTOR pathway is central in regulating key cellular processes such as proliferation, survival, metabolism, and angiogenesis. Dysregulation of this pathway, particularly in the AKT2 isoform, is commonly observed in cancers such as breast, ovarian, and pancreatic cancers, leading to enhanced tumor progression, metastasis, and therapeutic resistance. Therefore, targeting AKT2 for inhibition is a promising strategy for cancer therapy. This study utilized molecular docking and dynamics simulations to identify natural phytochemicals that inhibit AKT2. Molecular docking results revealed that millettone (CID 442810) exhibited the highest binding affinity to AKT2, with a docking score of −9.5 kcal/mol, followed by uzarigenin (CID 92760), dihydrobiochanin A (CID 439784), and abyssinone I (CID 442152) with docking scores of −9.0 kcal/mol, −8.9 kcal/mol, and −8.7 kcal/mol respectively, outperforming the control inhibitor, ipatasertib (CID 24788740) docking score of −7.56 kcal/mol. Molecular dynamics simulations indicated that millettone, uzarigenin, and dihydrobiochanin A demonstrated strong binding affinities and stable interactions with AKT2, suggesting their potential as therapeutic agents for cancers that involve AKT2 hyperactivation. Notably, uzarigenin's superior stability, as evidenced by its lower root mean square deviation (RMSD), which measures structural stability, and solvent-accessible surface area (SASA), which indicates molecular compactness, highlights its promise as a potent inhibitor of AKT2. Future in vitro and in vivo studies will be crucial to confirm the efficacy of these inhibitors in reducing tumor progression and their potential applications. Given that AKT2 also plays a role in neuronal survival and plasticity, these compounds may have potential applications in neurodegenerative diseases such as Alzheimer's, warranting further investigation into their dual therapeutic relevance.

1. Introduction

The AKT, also known as Protein Kinase B (PKB), is a crucial signal transduction pathway involved in regulating various cellular processes, including proliferation, survival, metabolism, and angiogenesis. These processes are fundamental to both normal cell physiology and pathological conditions such as cancer [1,2]. In cancer, the PI3K/AKT/mTOR signaling pathway is often dysregulated,

* Corresponding author.
E-mail address: aghosh-bmb@sust.edu (A. Ghosh).

https://doi.org/10.1016/j.heliyon.2025.e41897
Received 9 November 2024; Received in revised form 9 January 2025; Accepted 9 January 2025
Available online 10 January 2025

leading to uncontrolled cell growth, survival, proliferation, and resistance to apoptosis [3]. Mutations in upstream regulators such as PI3K catalytic subunit alpha (*PIK3CA*) or the tumor suppressor phosphatase and tensin homolog (*PTEN*), which normally acts as a negative regulator of AKT, can result in the constitutive activation of AKT [4]. This hyperactivation of the AKT pathway leads to enhanced tumor progression, increased metastatic potential, and resistance to various cancer therapies, making it a prime target for therapeutic interventions [5]. In particular, the three isoforms of AKT—AKT1, AKT2, and AKT3—are differentially involved in various cancer types [6]. AKT2, for instance, plays a critical role in regulating glucose metabolism and cell survival and is frequently overexpressed or hyperactivated in cancers such as breast, ovarian, and pancreatic cancers [7]. This isoform's significant contribution to tumor cell survival, invasion, and metastasis has driven considerable interest in identifying inhibitors that specifically target AKT2 to improve therapeutic outcomes in these malignancies [8].

Inhibitors targeting the PI3K/AKT/mTOR pathway have shown promise in preclinical and clinical studies, either as monotherapies or in combination with other anticancer agents. These inhibitors are designed to block the phosphorylation of AKT or interfere with its activation or downstream signaling [9,10]. One class of inhibitors includes small molecules such as perifosine, MK-2206, and ipatasertib, which directly inhibit AKT by binding to its ATP-binding pocket [11]. These inhibitors have shown potential in treating a variety of cancers, including breast, prostate, and lung cancers. For example, perifosine, a lipid-based inhibitor, disrupts AKT membrane localization and subsequent activation, leading to cell death in cancer cells. Similarly, MK-2206, a non-ATP-competitive inhibitor, prevents AKT phosphorylation and activation, thereby inhibiting its pro-survival signaling pathways [7,12–15]. Moreover, dual inhibitors that target both phosphoinositide 3 kinase (PI3K) and mammalian target of rapamycin (mTOR), such as BEZ235, have been developed to block the entire PI3K/AKT/mTOR axis [16]. This approach provides a broader therapeutic effect by inhibiting multiple components of the pathway, potentially overcoming the compensatory mechanisms that often lead to drug resistance [17]. While these inhibitors hold promise, there are challenges related to toxicity, off-target effects, and the development of resistance, which continue to complicate their clinical application [18].

In addition to synthetic inhibitors, natural compounds or phytochemicals have emerged as potential modulators of the AKT pathway. Phytochemicals are naturally occurring compounds found in plants, and many have demonstrated anticancer properties by modulating key signaling pathways, including the PI3K/AKT/mTOR pathway. These compounds are particularly attractive due to their relatively low toxicity and pleiotropic effects [19,20], which allow them to target multiple molecular pathways simultaneously [21–23].

Phytochemicals, such as curcumin, quercetin, and resveratrol, have shown significant promise in targeting key components of the PI3K/AKT/mTOR pathway [24]. These naturally occurring compounds possess anticancer properties that inhibit tumor growth and progression, providing a compelling alternative to synthetic inhibitors [24]. Phytochemicals have garnered attention as potential AKT2 inhibitors due to their natural origin and therapeutic properties. For instance, compounds such as saponin C, oleanolic acid, spinasterol, 20-hydroxyecdysone, and ecdysone, derived from *Achyranthes aspera*, have demonstrated inhibitory effects against AKT2 in molecular docking studies [25]. Additionally, honokiol, a bioactive biphenolic phytochemical, has been reported to inhibit AKT activity, contributing to its anticancer effects. These examples underscore the potential of phytochemicals as viable alternatives to synthetic inhibitors in targeting AKT2 for cancer therapy [26].

Given the potential of phytochemicals in cancer therapy, there has been growing interest in exploring their use as complementary or alternative treatments to existing anticancer therapies. Moreover, phytochemicals can be used in combination with existing therapies to enhance treatment efficacy and overcome drug resistance [27,28]. Cancer cells often develop compensatory mechanisms to bypass the inhibition of AKT, either by activating alternative signaling pathways or by mutating the target proteins themselves. This resistance can reduce the efficacy of AKT inhibitors and limit their long-term success in cancer treatment [29].

The AKT pathway plays a pivotal role in cancer development and progression, making it an attractive target for therapeutic intervention. However, challenges such as drug resistance, toxicity, and selectivity remain, necessitating further research into more effective and targeted therapies. This study aims to explore the therapeutic potential of targeting key molecules within the AKT pathway to enhance treatment specificity and safety in cancer therapy. Through molecular docking and simulation, various therapeutic agents were identified that interact with critical components of the AKT pathway by revealing their inhibitory effects. These findings offer promising insights for developing novel treatments and underscore the need for continued research to validate these approaches and advance innovative therapies for improved cancer outcomes.

2. Materials and methods

2.1. Ligand selection

Phytochemicals with known anticancer properties were selected from Dr. Duke's Phytochemical and Ethnobotanical Databases and PubChem. Compounds were prioritized based on documented anticancer activity from existing literature, and their availability in databases such as PubChem and Dr. Duke's Phytochemical and Ethnobotanical Databases. Moreover, flavonoids and terpenoids are the most used phytochemicals for cancer treatment and were chosen to target various pathways relevant to cancer progressions, such as ERK, PKC, and PI3K/AKT signaling pathway, which is a critical driver of tumor growth and survival [30]. This focused approach aimed at identifying ligands with a higher likelihood of inhibiting AKT2, as these pathways are directly involved in its activation and downstream pro-survival signaling. Each ligand's structure was retrieved from the PubChem database, and the corresponding 3D structures were downloaded in SDF format.

2.2. Protein selection

The three-dimensional structure of the (PKBbeta/Akt-2) complexed with isoquinoline-5-sulfonic acid (2-(2-(4-chlorobenzyloxy) ethylamino)ethyl)amide (PDB ID: 2JDO) was retrieved from the Protein Data Bank (PDB) [31]. The AKT2 protein structure selected for this study contained a well-characterized binding site essential for accurate molecular docking. The protein was prepared for docking by removing all bound ligands' water molecules and adding polar hydrogen atoms.

2.3. Active site prediction

The active site of AKT2 was predicted using CASTP v3.0 (http://sts.bioe.uic.edu/castp/calculation.html) to identify and measure potential ligand-binding pockets [32]. The key residues within the active site, as identified by CASTP, were validated by cross-referencing with the binding site from the PDB structure to ensure accurate prediction. This tool provided detailed information on the active sites, including the names and numbers of the residues involved. These active sites are critical regions on the protein where ligands, such as the selected phytochemicals, can bind. This site was further confirmed by superimposing known AKT2 inhibitors.

2.4. ADMET profiling

ADMET (Absorption, Distribution, Metabolism, Excretion, and Toxicity) profiling was performed on the selected phytochemicals using the SwissADME (http://www.swissadme.ch/index.php) and pkCSM (https://biosig.lab.uq.edu.au/pkcsm) tools [33,34]. Only compounds meeting the following thresholds were selected for docking studies: molecular weight between 120 and 500 g/mol, rotatable bond count between 1 and 10, heavy atom count between 12 and 30, hydrogen bond donors and acceptors each between 0 and 10, and polar surface area between 4.9 and 104 $Å^2$. Additional criteria included XLOGP between 1 and 5, positive blood-brain barrier (BBB) permeability, no violations of Lipinski's rules indicating that the compounds meet the criteria for drug-likeness, including a molecular weight $\leq$500 g/mol, a LogP value $\leq$ 5, no more than 5 hydrogen bond donors, and no more than 10 hydrogen bond acceptors. These guidelines are widely used to predict good absorption and permeation, ensuring that the selected compounds have favorable pharmacokinetic properties for oral bioavailability and negative results for AMES toxicity, hepatotoxicity, and skin sensitization (Table 1).

2.5. Molecular docking at the active site

The selected compounds that passed ADMET profiling were chosen for molecular docking studies using PyRx 0.8 (https://pyrx.sourceforge.io) [35]. Ligands were energy-minimized using Open Babel within the PyRx suite by employing the steepest descent algorithm and the Universal Force Field (UFF). The target protein was converted into pdbqt format, Water molecules were removed from the protein structures using pyMol (https://www.pymol.org/), and then the polar hydrogens were added to ensure proper protonation states of amino acid residues. This step was carried out using PyRx, an integrated virtual screening tool widely used for molecular docking studies. PyRx employs AutoDock tools for receptor preparation, ensuring the addition of polar hydrogens and assignment of partial atomic charges using the Gasteiger algorithm. This preparation step ensures the accurate modeling of interactions between ligands and the active site of the receptor during docking analysis. A grid box was defined around the active site to ensure optimal ligand binding. The dimensions of the grid box ($x = 47.999$, $y = 59.779$, $z = 56.357$) were chosen to encompass the entire binding pocket, providing sufficient coverage to accommodate ligands of varying sizes and ensuring all key residues within the active site were included. The center coordinates of the grid box ($x = 18.886$, $y = 3.501$, $z = -2.222$) were determined based on structural data and known functional regions of the target protein to maximize docking accuracy. The exhaustiveness value was set to 8, a commonly used parameter in molecular docking that balances computational efficiency with the thorough exploration of binding poses. This value ensures a reliable sampling of potential ligand conformations and orientations. Docking was performed in triplicate to ensure consistency, and the results were expressed in kcal/mol, with more negative values indicating stronger binding affinity. The top-ranked phytochemicals were analyzed for their interaction with key residues in the AKT2 active site, focusing on hydrogen bonding, hydrophobic interactions, and π-π stacking. Visualization of docked complexes was performed using Biovia Discovery Studio and PyMol to illustrate the molecular interactions.

2.6. Decoy screening of phytochemicals

Ligands that demonstrated better binding affinities than the positive control were selected for decoy screening to assess their specificity. The SMILES strings of these ligands were first generated and then input into the DUDE server (https://dude.docking.org), which provided corresponding decoy molecules [36]. These decoys are structurally like active ligands but are designed to avoid specific interactions with the target protein. In the generator option, each of the phytochemicals has 50 unique compounds which are considered as a negative control for each of the sorted chemicals. The decoy SMILES strings were downloaded in text format and converted into 3D molecular structures using Open Babel software, resulting in SDF files [37]. These 3D decoy structures were then docked with the target protein using the same docking protocols applied to the active ligands. The docking results, including binding affinities, were retrieved in CSV format. By comparing the binding affinities of the decoys to those of the active ligands, the specificity of the inhibitors was assessed, helping to validate the docking outcomes and ensure the reliability of the identified inhibitors.

Table 1
AMDET profiling parameters and shorting criteria.

Molecular Weight g/mol [Min-Max]	Rotatable Bond Count [Min-Max]	Heavy Atom Count [Min-Max]	H-Bond Donor Count [Min-Max]	H-Bond Acceptor Count [Min-Max]	Polar Area, [Angstrom sq] [Min-Max]	Complexity [Min-Max]	XLOGP [Min-Max]	BBB permeability	Rules 5	Hepatotoxicity	AMES toxicity
120–500	1–10	12–30	0–10	0–10	4.9–104	144–494	1–5	Yes	No violation	No	No

2.7. Molecular dynamics (MD) simulation

Molecular dynamics simulations were conducted using GROMACS v2020.6 to assess the stability of the AKT2-ligand complexes over a simulation time of 100 ns. The CHARMM36 force field was employed, and the TIP3P water model was used to solvate the system. Ions were added to neutralize the system, and energy minimization was performed to remove any steric clashes. The system underwent NVT (isothermal-isovolumetric) equilibration for 100 ps and NPT (isothermal-isobaric) equilibration for 100 ps. The production MD simulation was then run for 100 ns. The root mean square deviation (RMSD), root mean square fluctuation (RMSF), radius of gyration (Rg), solvent accessible surface area (SASA), principle component analysis (PCA), and covariance were calculated to assess the stability and compactness of the complexes over time.

2.8. Visualization of results

Visualization of the molecular docking and simulation results were performed using Biovia Discovery Studio and PyMol. The docked complexes were visualized to highlight key binding interactions, including hydrogen bonds, hydrophobic interactions, and electrostatic interactions between the phytochemicals and AKT2. The MD simulation trajectories were analyzed to illustrate the time-dependent conformational changes and binding stability of the complexes.

2.9. Metabolic pathway analysis

Metabolic pathway analysis was performed using the Kyoto Encyclopedia of Genes and Genomes (KEGG) (https://www.genome.jp/kegg/pathway.html). The analysis focused on the involvement of AKT2 in cancer-related pathways such as cell survival, apoptosis, and proliferation. The pathways were illustrated in a detailed map showing how AKT2 influences downstream targets in the PI3K/AKT/mTOR pathway and its role in various cancers.

3. Result

3.1. Ligand selection

Phytochemicals like terpenoids, their derivatives, and the bioactive compounds from Dr Duke's database were selected as primary ligands for inhibiting AKT protein. Initially, 729 phytochemicals were identified. After removing duplicates, 526 unique compounds remained, which CID and canonical smiles have retrieved from the PubChem database for further analysis. Ipatasertib (CID 24788740), a well-known AKT inhibitor, was selected as the positive control for comparison during the initial screening. As a clinically relevant AKT inhibitor, Ipatasertib provides a benchmark to evaluate the binding affinity and efficacy of the screened phytochemicals [38].

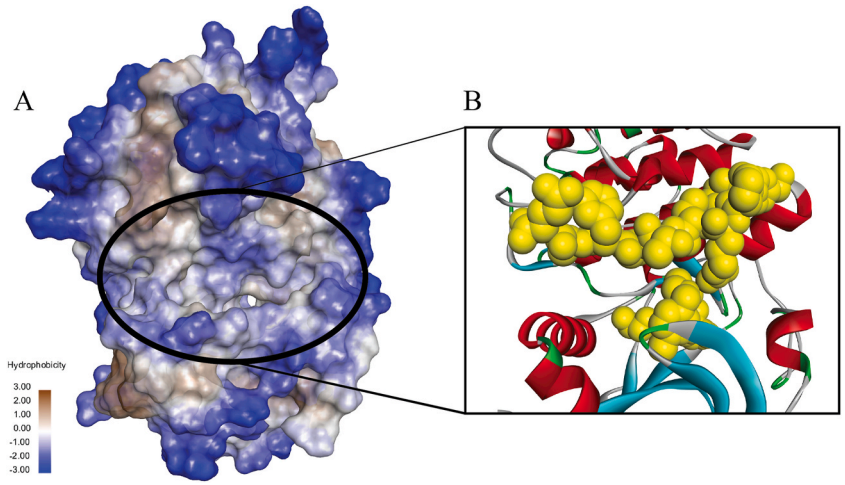

Fig. 1. Hydrophobicity mapping and molecular interaction of the protein-ligand complex. (A) Surface representation of the protein, color-coded according to hydrophobicity (scale bar shown to the left). Blue indicates hydrophilic regions, while brown indicates hydrophobic areas. The region of interest, likely a binding site, is circled. (B) Magnified view of the circled binding site showing the ligand (yellow spheres) interacting with specific residues of the protein (shown as ribbon representation). Red helices, brown loops, and blue beta-sheets illustrate the secondary structure of the protein. The binding interactions between the ligand and the hydrophobic pocket are emphasized.

3.2. Prediction of active sites for AKT

The CASTp has identified an active site of 761.594 $Å^2$ Area and a volume of 483.585 $Å^3$ (Fig. 1A). These values are consistent with reported sizes for kinase active sites, which typically range between 400 and 800 $Å^3$ in volume. These dimensions are slightly larger than the average for kinases like EGFR (~450 $Å^3$) but smaller than larger kinases such as CDK2 (~600 $Å^3$), suggesting a moderate-sized binding pocket well-suited for accommodating diverse ligands (Fig. 1B). Including these contextual comparisons highlights the suitability of the AKT2 active site for targeted inhibitor design [39,40]. The active site residues consist of hydrophobic amino acids which facilitate hydrophobic interactions essential for ligand binding (Fig. 1A). Polar residues contribute to hydrogen bonding, while charged residues enable electrostatic interactions (Table S1). Additionally, aromatic residues may support π-π stacking interactions. Together, these residues play a crucial role in stabilizing the ligand binding within the active site through a combination of hydrophobic, polar, and charged interactions, contributing to the protein's function and potential inhibition by ligands (Table 2).

3.3. ADMET profiling of sorted phytochemicals

ADMET profiling was performed for the 526 phytochemicals sorted. The compounds were analyzed further for some threshold points such as poor absorption or permeation is expected to occur more frequently in the discovery setting when the number of H-bond donors exceeds 5, the number of H-bond acceptors reaches 10, the molecular weight (MWT) exceeds 500, and AMES toxicity and hepatotoxicity should be negative [41]. Most of the phytochemicals did not satisfy the threshold point that was sought for further analysis. Among the total of 526 compounds, only 90 phytochemicals were filtered according to the threshold point. Compounds met criteria such as polar surface area, XLOGP, heavy atom count, rotatable bonds, etc., but many failed due to GI absorption, BBB permeability, AMES toxicity, hepatotoxicity, or violations of Lipinski's rules. The control compound, despite high GI absorption and BBB permeability, displayed hepatotoxicity and a Lipinski rule violation, limiting its potential as a drug candidate. Out of the total screened ligands, 214 failed due to poor GI absorption, 195 due to BBB permeability, 12 due to Lipinski's rule violations, and 15 due to hepatotoxicity and AMES toxicity. In contrast, all phytochemicals demonstrated high GI absorption without hepatotoxicity, satisfying essential ADMET criteria for drug discovery. For parameters such as heavy atoms, rotatable bonds, and molecular flexibility, most phytochemicals displayed better drug-like properties compared to Ipatasertib (Table S2).

The other parameters of ADMET profiling results such as heavy atoms, rotatable bonds, h-bond acceptors, H-bond donors, max. tolerated dose (human), skin sensitization, and minnow toxicity were also analyzed (Data set S1). All these findings suggest that these compounds are suitable for further examination through docking and stability testing.

3.4. Molecular docking at the active site

The ADMET-filtered phytochemicals, along with the positive control, were further analyzed through docking in triplicates using PyRx (Table S3). For each ligand, the binding energy values from the triplicate docking runs were averaged, and the standard deviation was calculated to evaluate consistency across the docking simulations. The top 5 Phytochemicals with a higher binding affinity than the positive control were considered potential inhibitors, and their interacting residues were analyzed further. The docking analysis of various compounds against AKT2 (PDB: 2JDO) revealed distinct interactions and binding affinities. Additionally, a decoy set was used to compare the docking results, ensuring the validity of the docking scores and interactions. Ipatasertib, a control AKT2 inhibitor, showed a binding affinity of −7.56 kcal/mol, interacting via hydrogen bonds with Lys128, Asn151, and Gly22, as well as hydrophobic interactions with Val105. The highest binding affinity of the decoy set for AKT2 was −7.2 kcal/mol, confirming that the ligands under investigation outperformed the decoys (Table 3).

The comparative analysis of docking results revealed that millettone had the highest binding affinity of −9.5 kcal/mol with AKT2, exactly same to its decoy, interacting hydrophobically with Val105, Ile24, Lys128, and Ala126, and forming hydrogen bonds with Asn209 and Glu162. Uzarigenin also demonstrated strong inhibition with a binding affinity of −9.0 kcal/mol, interacting hydrophobically with Val105 and forming hydrogen bonds with Asn209, Gly47, Gly48, Ala49, and His50. Other potent inhibitors included Dihydrobiochanin A with a binding affinity of −8.9 kcal/mol, interacting with residues such as Trp203, Val105, Met205, and forming hydrogen bonds with Asn151, Asn218, and Lys128. Abyssinone I exhibited a binding affinity of −8.7 kcal/mol, also outperforming its decoy counterpart (−9.0 kcal/mol), interacting hydrophobically with Ile24, Ala126, Met267, and forming hydrogen bonds with His200, Glu153, Trp203, and Met205. Sainfuran showed a binding affinity of −8.6 kcal/mol, interacting with residues like Gln222, Lys128, Ser127, Asn218, and Ser245, and forming hydrogen bonds with Ala126, His200, and Glu153. The docking results, in comparison to the decoy set, confirmed that the tested compounds demonstrated stronger binding affinities, validating them as potential

Table 2
Classification of active site residues and their roles in ligand binding.

Residue Type	Residues Identified	Role in Ligand Binding
Hydrophobic Residues	ILE, VAL, LEU, ALA, MET	Facilitate hydrophobic interactions essential for ligand binding.
Polar Residues	THR, SER, ASN, GLN	Contribute to hydrogen bonding with ligands.
Charged Residues	LYS, GLU	Enable electrostatic interactions with ligands.
Aromatic Residues	HIS	Support π-π stacking interactions, stabilizing ligand binding.

Table 3
The Docking affinity with corresponding decoy and interacting residues.

Sl no	Chemical	CID	Docking Score (PyRx) (Kcal/mol)	Highest affitnity of decoy (PyRx) (Kcal/mol)	Hydrophobic Interaction	Bond Distance (Å)	Hydrogen/ Electrostatic Bond	Bond Distance (Å)
1	Ipatasertib (control)	24788740	−7.56 ± 0.5	−7.2	Lys128	5.46	Asn151	2.64
					Val105	4.39	Lys128	2.33
					Val105	4.33	Asn151	2.53
							Gly22	3.47
2	Millettone	442810	−9.5 ± 0	−9.5	Val105	3.85	Asn209	2.52
					Ile24	5.14		
					Lys128	3.97	Glu162	3.79
					Ala126	5.49		
3	Uzarigenin	92760	−9.0 ± 0	−7.9	Val105	4.42	Asn209	2.83
							Gly47	1.81
							Gly48	2.97
					His50	5.29	Ala49	2.38
							His50	2.26
							His50	2.32
4	Dihydrobiochanin A	439784	−8.9 ± 0	−6.0	Trp203	5.28	Lys128	3.04
					Val105	3.99		
					Met205	5.33	Asn151	2.81
					Ala126	4.70	Asn218	1.98
5	Abyssinone I	442152	−8.7 ± 0.5	−9.0	Ile24	3.99	His200	2.49
							Lys219	4.94
					Ala126	5.21	Glu153	3.26
							Trp203	3.02
					Met267	3.95	Met205	3.62
6	Sainfuran	185034	−8.6 ± 0.0	−8.2	Gln222	2.16	Ala126	3.70
					Lys128	2.61	Ala176	4.31
					Ser127	2.67	Met205	4.27
					Asn218	3.07	His200	3.50
					Ser245	2.08	Glu153	3.24
					Ala126	2.50	Ile24	4.68
							Lys219	5.20
							Glu153	4.81

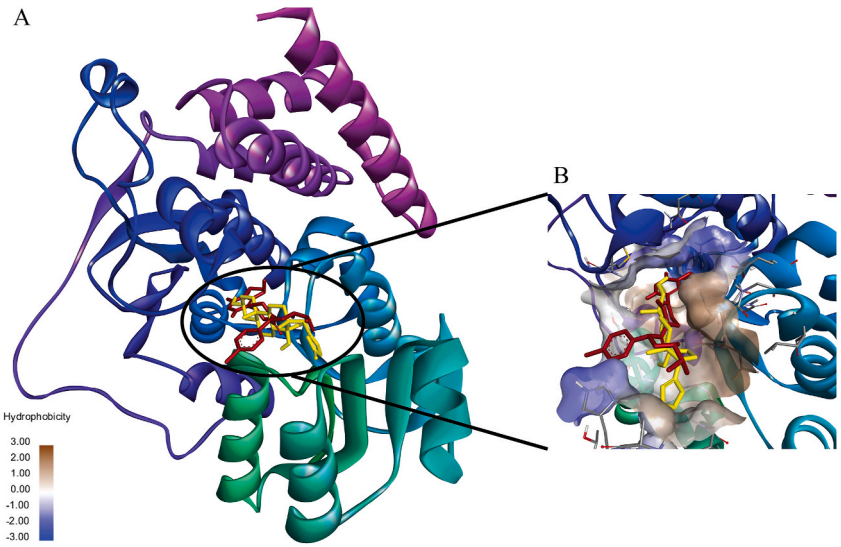

Fig. 2. An illustration of the AKT protein binding with ipatasertib and uzarigenin. (A) a zoomed-out view of the AKT protein, highlighting the binding pocket where both ligands are positioned. The spatial alignment of the two ligands indicates their similar occupancy within the active site. (B) zoomed-in view of the same binding pocket, with the surface color-coded by hydrophobicity, where brown represents hydrophobic regions and blue represents hydrophilic regions. This hydrophobicity mapping provides insight into the interactions that contribute to the stability of the ligands within the binding site. Uzarigenin (yellow), which was selected for further analysis due to its superior simulation results, occupies a similar position as ipatasertib (red) and interacts effectively with both hydrophobic and hydrophilic regions, as visualized in this surface representation.

inhibitors. Interactions with critical residues like Val105, Lys128, and Asn209 were essential for binding, particularly in inhibitors with higher affinities. These residues emerged as crucial targets for enhancing inhibitory potential, and the comparison with the decoy results further strengthens the evidence of these compounds' effectiveness (Fig. S1).

3.5. Molecular dynamics simulation analysis

A 100-ns molecular dynamics (MD) simulation was conducted to assess the stability of ligand-protein interactions in the AKT protein, with the primary ligands being ipatasertib (CID 24788740) as the control and uzarigenin (CID 92760) as the test compound. Uzarigenin was specifically chosen for detailed analysis because it exhibited better stability and favorable simulation results in comparison to other tested ligands. The analysis utilized key metrics such as RMSD, RMSF, SASA, and Rg to evaluate the dynamic behavior and compactness of the ligands in their respective binding sites. The spatial comparison of the binding grooves revealed that both ligands occupied similar pockets within the protein (Fig. 2A), but only complexes with superior performance in these metrics were considered for further evaluation. Uzarigenin demonstrated interactions comparable to the control ligand, maintaining effective positioning in the hydrophobic pocket (Fig. 2B). The surface representation, color-coded by hydrophobicity, revealed that both ligands interacted with hydrophobic and hydrophilic regions, with brown areas indicating hydrophobic zones and blue areas marking hydrophilic zones. Uzarigenin effectively occupied the same pocket as ipatasertib, and although the MD simulation revealed slightly higher RMSD values for Uzarigenin, indicating increased fluctuation, its overall binding stability was sufficient to warrant further investigation. This is why Uzarigenin was chosen to visualize the interaction within the binding pocket.

A 100-ns molecular dynamics (MD) simulation was performed to assess the stability of protein-ligand interactions with AKT for two ligands: ipatasertib as the control and uzarigenin (CID 92760) as the test compound. The stability of the complexes was evaluated through root means square deviation (RMSD) and root means square fluctuation (RMSF) analyses. The RMSD for the AKT protein bound with ipatasertib shows relatively stable values for the protein, fluctuating between 0.3 and 0.5 nm over the 100 ns simulation.

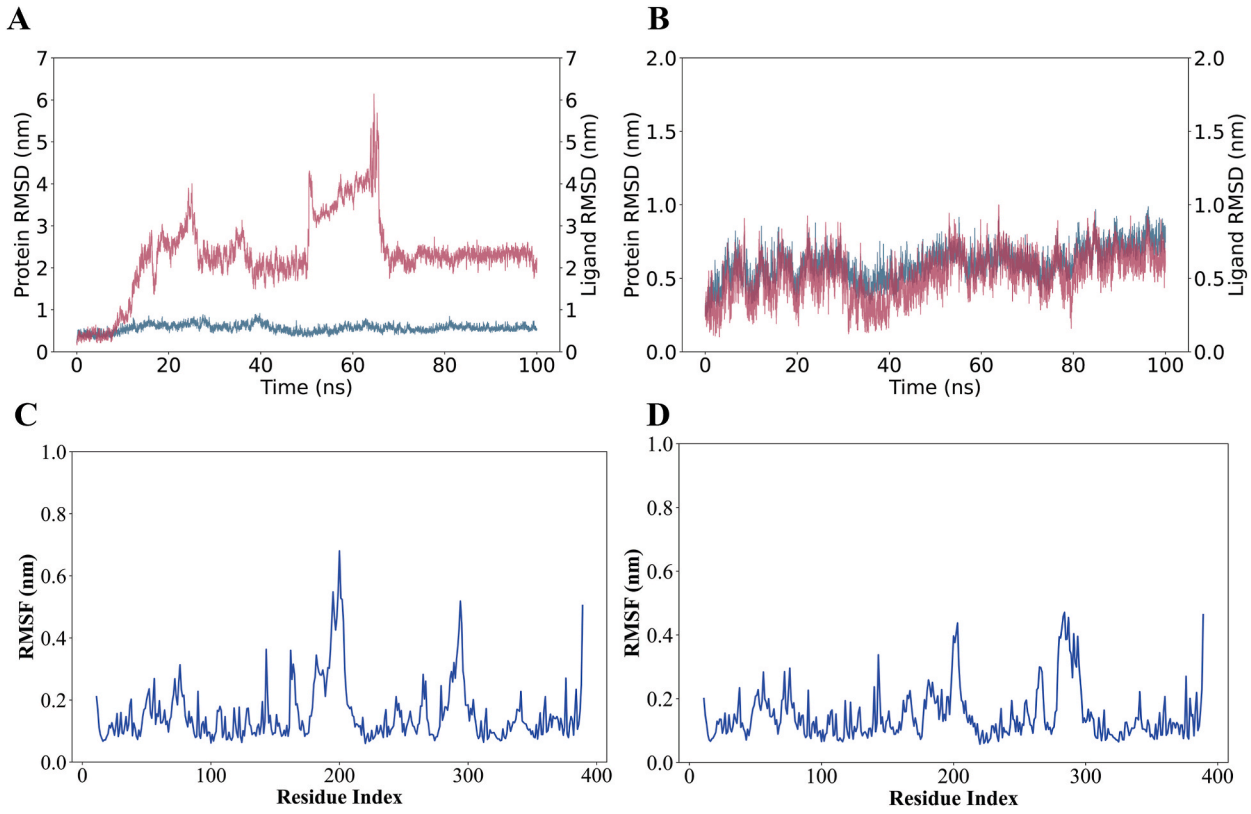

Fig. 3. RMSD and RMSF analyses of AKT protein interactions over 100 ns. (A) the root means square deviation (RMSD) analysis of the AKT protein (blue) and the ligand ipatasertib (red) over 100 ns time scale. The protein shows stable behavior with RMSD fluctuating between 0.3 and 0.5 nm, while the ligand shows significant fluctuations, reaching up to 6.0 nm at 60–70 ns, before stabilizing around 3.0 nm, indicating unstable ligand binding. (B) The RMSD analysis of the AKT protein (blue) and the ligand uzarigenin (red). The protein remains stable with RMSD values between 0.2 and 0.5 nm, while the ligand shows moderate fluctuations between 0.5 and 1.0 nm, indicating more stable binding compared to ipatasertib. (C) RMSF profile of the AKT protein bound to ipatasertib. Significant fluctuations are observed around residues 200–250 and 300–350, indicating flexible regions of the protein upon ligand binding. (D) RMSF profile of the AKT protein bound to Uzarigenin shows lower fluctuations in general, with peaks around residues 200–300, suggesting that Uzarigenin induces less conformational flexibility in the protein compared to Ipatasertib.

However, the ligand (Ipatasertib) shows substantial deviations, with its RMSD increasing up to 6.0 nm around the 60–70 ns mark, before stabilizing at a value close to 3.0 nm. This suggests significant movement or flexibility of the ligand during the simulation, indicating weaker binding interactions with the protein over time (Fig. 3A). On the other hand, uzarigenin is more stable compared to ipatasertib, with the protein RMSD fluctuating between 0.2 and 0.5 nm. The ligand (Uzarigenin) shows consistent stability throughout the simulation, with RMSD values ranging between 0.5 and 1.0 nm, indicating stronger and more consistent binding compared to the control ligand (Fig. 3B). The RMSF analysis for the AKT protein bound with ipatasertib indicates significant fluctuations, particularly around residues 200–250 and 300–350, where the values reach up to 0.8 nm. These fluctuations suggest that the binding of ipatasertib induces some level of conformational flexibility in the protein, especially in the active site (Fig. 3C). In contrast, the RMSF analysis for the AKT protein bound with uzarigenin shows lower fluctuations, generally around 0.2–0.4 nm, with minor peaks around residues 200–300. This suggests that uzarigenin induces a less conformational change in the protein, implying a more stabilizing effect on the AKT structure compared to ipatasertib (Fig. 3D).

The RMSD and RMSF analysis collectively indicate that uzarigenin demonstrates stronger and more stable binding to the AKT protein compared to the control ligand, ipatasertib. While ipatasertib shows significant ligand movement and induces more fluctuations in the protein, uzarigenin displays more consistent behavior with less conformational flexibility, suggesting that it may have a more favorable binding profile with AKT. The RMSD analysis of the AKT and Millettone shows that the protein remains stable with fluctuations between 0.3 and 0.5 nm, while the ligand displays significant changes, peaking around 2.0 nm, suggesting variable ligand stability (Fig. S2A). The RMSD of dihydrobiochanin A indicates that the protein remains stable, fluctuating between 0.2 and 0.5 nm, while the ligand shows larger fluctuations, reaching up to 5.0 nm, reflecting less stable ligand binding (Fig. S2B). Abyssinone I's RMSD shows moderate ligand stability with fluctuations between 0.5 and 3.0 nm, while the protein maintains a stable profile (Fig. S2C). Sainfuran displays the highest ligand RMSD fluctuations, reaching up to 5.0 nm, indicating unstable binding, while the protein remains stable (Fig. S2D). The other four ligand complexes have more deviation and fluctuations have been observed. The RMSF profiles for all ligands reveal varying degrees of protein flexibility, with peaks around residue regions 150–200 and 250–350, indicating that binding induces localized flexibility in the AKT protein (Figs. S2E–H).

The solvent-accessible surface area (SASA) and radius of gyration (Rg) analyses provide insight into the structural stability and compactness of the AKT protein-ligand complexes during a 100 ns MD simulation with ipatasertib and uzarigenin. The SASA values reveal differences in the solvent exposure of the protein surface for the two protein-ligand complexes. The AKT protein complexed with ipatasertib, where SASA fluctuates between 202 nm^2 and 208 nm^2. These fluctuations suggest some changes in surface exposure over the simulation, indicating a degree of flexibility in this complex, on the other hand, the AKT protein complexed with uzarigenin exhibits slightly lower SASA values, fluctuating between 198 nm^2 and 206 nm^2. This indicates a more compact and less exposed structure compared to the ipatasertib complex, implying that uzarigenin interacts more tightly with the protein, reducing the surface area available for solvent interaction (Fig. 4A).

The Rg measures the overall compactness of the protein-ligand complexes. The Gyration value of ipatasertib has ranged between 2.10 nm and 2.20 nm, suggesting slight fluctuations in the protein's compactness. The increase in Rg up to 50 ns indicates some expansion in the protein structure before stabilizing in the latter half of the simulation. The complex with uzarigenin shows more compact Rg values, fluctuating between 2.05 nm and 2.17 nm, suggesting that this complex maintains a more compact and stable structure throughout the simulation. This lower Rg indicates stronger binding and reduced flexibility of the protein when bound to Uzarigenin compared to ipatasertib. The SASA and Rg analyses suggest that the uzarigenin complex maintains a more compact and stable structure with lower solvent exposure, indicating tighter binding and less flexibility (Fig. 4B). In contrast, the ipatasertib

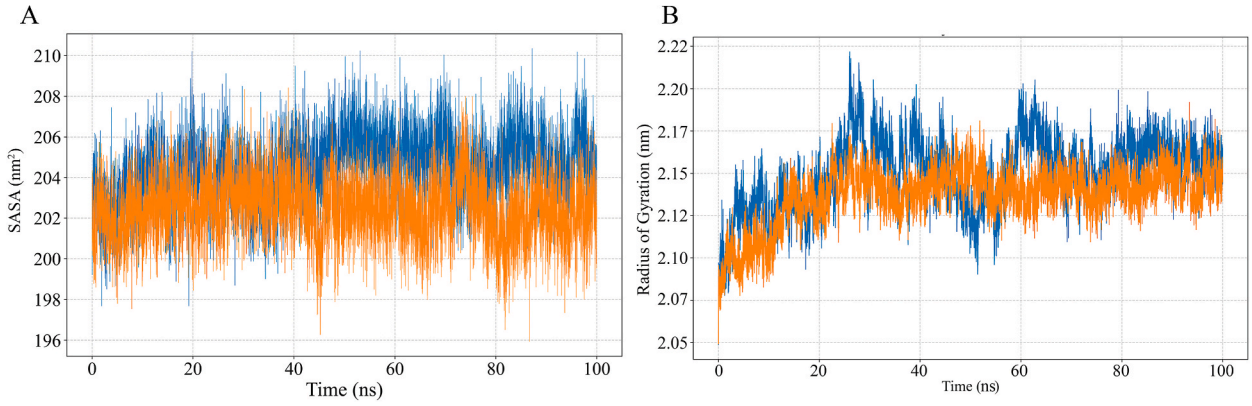

Fig. 4. Solvent Accessible Surface Area (SASA) and Radius of Gyration (Rg) analyses of AKT protein-ligand complexes over a 100 ns simulation. (A) SASA analysis shows surface exposure of the AKT protein-ligand complexes, with the ipatasertib complex (blue) exhibiting higher SASA values (~204–208 nm^2), indicating greater solvent exposure, while the uzarigenin complex (orange) maintains lower SASA values (~200–204 nm^2), suggesting a more compact conformation. (B) Radius of Gyration (Rg) analysis reveals that the ipatasertib complex has slightly higher Rg values (~2.15–2.20 nm), reflecting a more expanded structure, whereas the uzarigenin complex consistently shows lower Rg values (~2.12–2.16 nm), indicating a more compact and stable protein-ligand interaction. Together, these results suggest that uzarigenin promotes a tighter and more stable binding conformation compared to ipatasertib.

complex shows higher SASA and Rg values, suggesting a more exposed and flexible structure. These results imply that Uzarigenin forms a more stable and stronger interaction with AKT compared to ipatasertib, which could make it a more effective ligand in this context. The other complexes SASA and Rg have also been analyzed further reveal structural instability within these complexes, suggesting a potential susceptibility to conformational fluctuations (Fig. S3).

3.6. PCA and dynamic covariance analysis

The principal component analysis (PCA) of the AKT protein complexed with uzarigenin reveals significant insights into the conformational dynamics of the system. The scatter plot of PC1 vs. PC2 shows that PC1 accounts for 14.61 % of the total variance, while PC2 explains 11.33 %. These two principal components highlight distinct conformational states of the protein-ligand interaction, with clear clustering of red and blue points indicating the sampling of different regions during the simulation. The PC1 vs. PC3 plot shows that PC3 contributes 7.22 % to the variance, suggesting additional conformational diversity within the complex. The combined variance of 33.16 % explained by the first three components indicates that these PCs capture most of the significant motions in the system, with PC1 dominating as the key contributor. The eigenvalue rank plot confirms that beyond the first few principal components, the explained variance decreases sharply, implying that a limited number of PCs are sufficient to describe the essential dynamics of the AKT-uzarigenin complex (Fig. 5A).

Dynamic Covariance analysis further complements the PCA by revealing the degree of correlation between residue movements within the AKT-Uzarigenin complex. The dynamic covariance (DC) (Fig. 5B) shows regions of both positive (red) and negative (blue) correlations, with moderate intensity. This suggests a balance between coordinated and independent residue movements, indicating that while Uzarigenin stabilizes certain regions of AKT through coordinated motions, other areas exhibit more independent dynamics. Compared to similar protein-ligand complexes, the covariance pattern here suggests that Uzarigenin induces moderate global stabilization but allows for considerable flexibility in specific regions of the protein, providing insight into its potential functional impact on AKT's dynamic behavior.

3.7. Metabolic pathway analysis

The metabolic pathway analysis of the AKT2 reveals significant involvement in cancer-related pathways and cellular signaling mechanisms. AKT2 proteins reveal, pathways such as the PI3K-Akt signaling pathway, commonly deregulated in cancers like breast

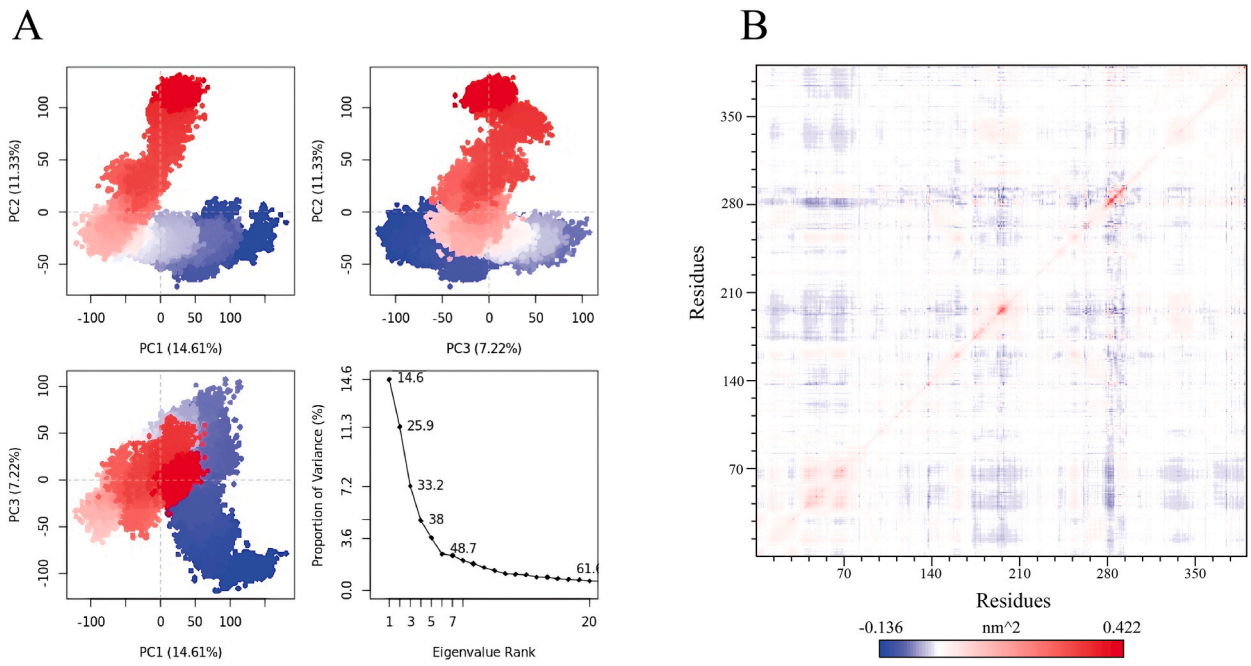

Fig. 5. Principal Component Analysis and Dynamic Covariance Matrix of the AKT-uzarigenin complex. (A) PCA scatter plots show the relationship between the first three principal components. The PC1 vs. PC2 plot shows PC1 explaining 14.61 % and PC2 explaining 11.33 % of the total variance, with distinct clustering of conformational states. The PC1 vs. PC3 plot shows that PC3 accounts for 7.22 % of the variance. The bottom-right panel displays the eigenvalue rank plot, highlighting the proportion of variance explained by each principal component, with PC1 contributing the most variance, followed by PC2 and PC3, together capturing 33.16 % of the system's total motion. (B) Covariance of residue motions in the AKT-Uzarigenin complex. Positive correlations (red) indicate residues moving in a coordinated manner, while negative correlations (blue) represent anticorrelated movements. The color intensity scale ranges from −0.136 to 0.422 nm^2, indicating varying degrees of correlation among residues across the protein complex.

cancer (HSA-05224) and colorectal cancer (HSA-05210), highlight the importance of AKT's function in regulating cell growth, survival, and metabolism. Dysregulation of AKT signaling contributes to uncontrolled cellular proliferation, resistance to apoptosis, and enhanced tumor survival, positioning this pathway as a major therapeutic target in oncology.

In addition to its role in cancer, the AKT is also linked to neurodegenerative pathways, particularly Alzheimer's disease (HSA-05010). Proteins like GSK3B, an essential player in tau phosphorylation and neurofibrillary tangle formation, interact with AKT in this context [42]. AKT's regulation of GSK3B activity is vital in controlling tau hyperphosphorylation, a hallmark of Alzheimer's pathology. Furthermore, pathways such as the neurotrophins signaling pathway (HSA-04722) underscore the relevance of AKT in neuronal survival and plasticity, suggesting that disruptions in AKT signaling could contribute to synaptic dysfunction and neuronal death observed in neurodegenerative diseases (Table 4).

4. Discussion

AKT2 is a critical isoform of the *AKT* family, heavily implicated in cancers such as breast, ovarian, and pancreatic cancers. Targeting AKT2 has been a focal point in cancer therapy due to its role in regulating cell survival, metabolism, and proliferation [43,44]. Hyperactivation of AKT2, often caused by mutations in upstream regulators like PI3K or loss of PTEN function, leads to tumor growth, metastasis, and resistance to therapy [45]. This study focused on identifying natural compounds with inhibitory potential against AKT2 to mitigate its role in oncogenesis, which is vital for the development of effective cancer therapies [46]. Molecular docking studies revealed that the phytochemicals millettone, uzarigenin, and dihydrobiochanin A exhibited better binding affinities compared to the control compound ipatasertib, a known AKT2 inhibitor (Table 2). Notably, millettone showed the highest binding affinity (−9.5 kcal/mol) to AKT2, stabilizing its inactive form through interactions with Val105, Lys128, and Asn209. Decoy screening confirmed its specificity, minimizing off-target effects. Uzarigenin demonstrated superior stability in 100 ns MD simulations, with lower RMSD and RMSF values than ipatasertib, indicating reduced AKT2 fluctuation. SASA and Rg analyses, along with PCA results, highlighted uzarigenin's tighter, more stable binding, reinforcing its potential as a potent AKT2 inhibitor.

Cardiac glycosides, a class of compounds to which uzarigenin belongs, have demonstrated anticancer activities through the inhibition of the PI3K/AKT/mTOR signaling pathway. For instance, cerberin, a cardiac glycoside, has been shown to exert anticancer effects by inhibiting this pathway [47]. Lanatoside C, another cardiac glycoside, has been reported to induce cell cycle arrest and suppress cancer cell proliferation by targeting the PI3K/AKT/mTOR pathway. This suggests that compounds like uzarigenin may share similar mechanisms of action [48]. The PI3K/AKT/mTOR pathway is frequently activated in various cancers, making it a critical target for therapeutic intervention. Inhibitors of this pathway have shown promise in clinical trials, underscoring the therapeutic relevance of compounds that can modulate this signaling cascade [49,50].

The PI3K/AKT/mTOR pathway, the involvement of AKT and its downstream signaling mechanisms in various cellular processes such as cell cycle regulation, glucose metabolism, and survival is critical for understanding its role in cancer progression and neurological diseases [51](Fig. 6), the activation of AKT through receptor tyrosine kinases (RTKs) and its subsequent impact on multiple pathways including mTOR, IKK, and GSK-3β—illustrates how dysregulation of this pathway leads to pathological outcomes such as cancer, neurodegenerative diseases, and cardiovascular disorders [52,53]. The crucial role of AKT in cell survival and metabolism, with implications for therapeutic strategies that target dysregulation in disease states. Specifically, the activation of AKT inhibits pro-apoptotic factors such as BAD and promotes cell proliferation by regulating cell cycle proteins like cyclin D1 [1]. The AKT influences glucose metabolism via mTOR, a pathway often hyperactivated in cancer and metabolic disorders like Type 2 diabetes. The involvement of AKT in neurological diseases, such as Alzheimer's and bipolar disorder, can be seen through its interaction with GSK-3β (Fig. 6), a protein closely linked to neurodegenerative processes [54,55].

The results of this study align with previous research on phytochemicals like curcumin, quercetin, and resveratrol, which have shown potential in modulating the PI3K/AKT pathway and inhibiting cancer progression [56]. Several studies have highlighted the critical role of AKT2 in cancer progression, particularly in breast, ovarian, and pancreatic cancers. For instance, Vivanco and Sawyers (2002) demonstrated that AKT2 is often overexpressed in breast and ovarian cancer cells, where its hyperactivation leads to increased cell survival, enhanced metastatic potential, and resistance to apoptosis [57]. This overactivation is frequently linked to mutations in the PI3K pathway or loss of PTEN function, resulting in the constitutive activation of AKT2, driving tumor growth and poor patient outcomes. In pancreatic cancer, Cheng et al. (2017) provided insights into the role of AKT2 in promoting cancer cell invasion and metastasis. They showed that AKT2, through its regulation of glucose metabolism and cell survival pathways, contributes to the

Table 4
Associated Protein pathway of AKT protein.

Term ID	Term description	False discovery rate	Matching proteins in your network (labels)
hsa05213	Endometrial cancer	1.11E-13	PIK3CA, GSK3B, FOXO3, AKT2, PIK3R1, AKT1
hsa05215	Prostate cancer	1.12E-12	PIK3CA, GSK3B, FOXO1, AKT2, PIK3R1, AKT1
hsa04722	Neurotrophin signaling pathway	2.42E-12	PIK3CA, GSK3B, FOXO3, AKT2, PIK3R1, AKT1
hsa05210	Colorectal cancer	5.08E-11	PIK3CA, GSK3B, AKT2, PIK3R1, AKT1, PIK3CB
hsa05224	Breast cancer	1.02E-09	PIK3CA, GSK3B, AKT2, PIK3R1, AKT1, PIK3CB
hsa05226	Gastric cancer	1.02E-09	PIK3CA, GSK3B, AKT2, PIK3R1, AKT1, PIK3CB
hsa05010	Alzheimer disease	7.01E-08	PIK3CA, GSK3B, AKT2, PIK3R1, AKT1, PIK3CB
hsa05205	Proteoglycans in cancer	1.89E-07	PIK3CA, AKT2, PIK3R1, AKT1, PIK3CB
hsa04014	Ras signaling pathway	3.66E-07	PIK3CA, AKT2, PIK3R1, AKT1, PIK3CB

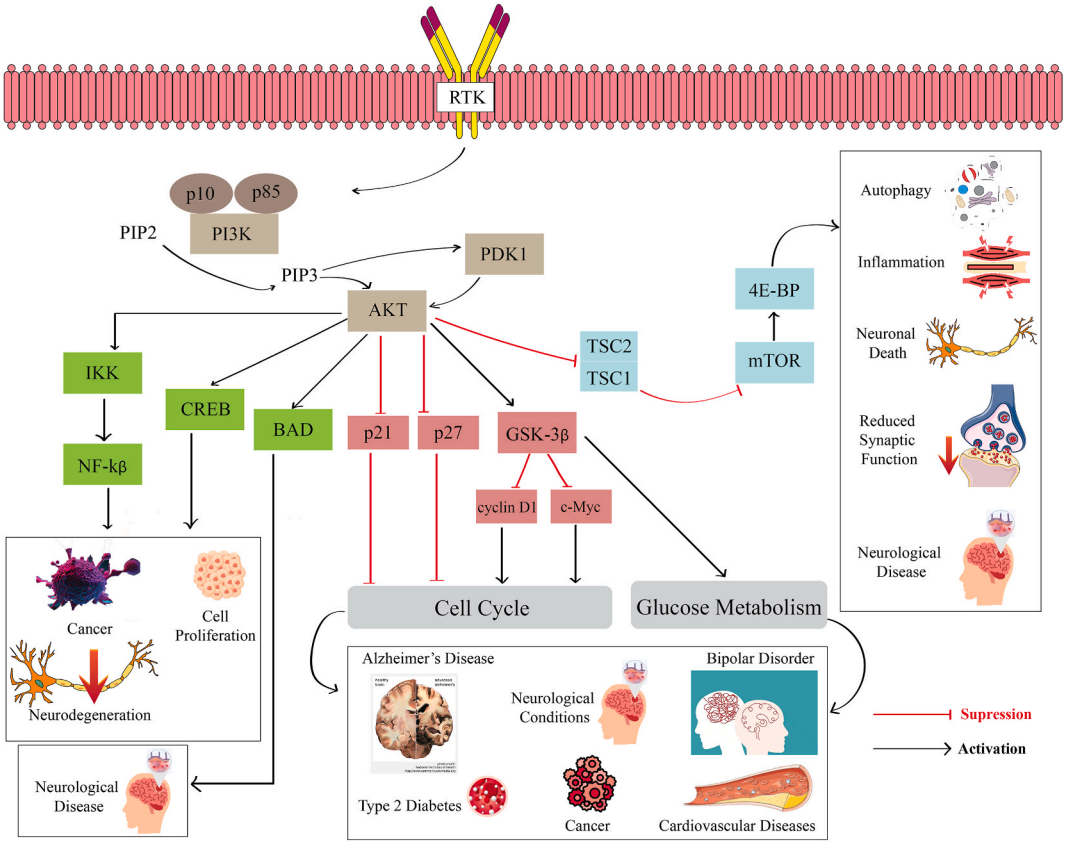

Fig. 6. Overview of the PI3K/AKT/mTOR Pathway and Its Role in Disease Progression. This figure illustrates the activation of the AKT pathway by receptor tyrosine kinases (RTKs) through the PI3K/PDK1 signaling cascade. Upon activation, AKT phosphorylates key downstream targets involved in processes such as cell cycle progression, glucose metabolism, and survival. Arrows indicate activation (solid black lines), while inhibitory effects are depicted with red lines and blunt-ended arrows. Key downstream components include mTOR, which regulates autophagy, inflammation, and neuronal death, and GSK-3β, which is linked to neurological diseases like Alzheimer's. AKT also inhibits apoptosis by phosphorylating pro-apoptotic proteins like BAD and activates survival pathways via NF-κB. Dysregulation of this pathway contributes to disease states, including cancer, neurodegenerative diseases, and metabolic disorders such as Type 2 diabetes. The color coding distinguishes pathway nodes: green for activated targets, red for inhibited components, and blue for regulatory intermediates. This schematic highlights the therapeutic potential of targeting specific pathway components for disease management.

aggressive nature of pancreatic cancer, making it a crucial target for therapeutic interventions aimed at reducing metastasis and improving patient survival [58]. Furthermore, the study by Altomare and Testa (2005) explored the PI3K/AKT pathway and highlighted AKT2's involvement in various malignancies, emphasizing its role in tumor cell invasion, resistance to apoptosis, and drug resistance [59]. These findings underline the significance of AKT2 as a therapeutic target, particularly for cancers that exhibit deregulated PI3K/AKT signaling. In terms of therapeutic development, several small molecule inhibitors have been developed to target the PI3K/AKT/mTOR pathway, including AKT2 [60,61]. Inhibitors like MK-2206 and ipatasertib directly target AKT2, demonstrating potential in reducing tumor growth by blocking AKT phosphorylation and subsequent downstream signaling [62]. However, challenges such as drug resistance and off-target effects remain prominent issues, prompting further research into alternative inhibitors, including natural compounds like phytochemicals [63,64].

Phytochemicals identified in this study, such as uzarigenin, offer a promising alternative to synthetic inhibitors due to their lower toxicity and potential to overcome limitations like drug resistance and poor selectivity. These compounds could complement existing therapies, enhancing efficacy in cancer treatment. Furthermore, the dual role of AKT2 in cancer and neurodegenerative diseases highlights the broader therapeutic applications of these inhibitors, including potential use in conditions like Alzheimer's. Future studies focusing on pharmacokinetics and in vivo efficacy will be critical to translating these findings into clinical applications. Uzarigenin's compact and stable binding profile, as observed through MD simulations, makes it an excellent candidate for further experimental validation. To substantiate these results, future research should include conducting kinase inhibition assays to measure the compounds' effects on AKT2 activity. For example, in vitro kinase assays have been used to evaluate the efficacy of AKT inhibitors in previous studies. Assessing the impact on cancer cell lines with overactive AKT2 to determine effects on cell proliferation and survival. Cell-based assays have been instrumental in understanding the role of AKT2 in cancer progression. Utilizing animal models to evaluate the therapeutic potential and safety profile of these compounds. In vivo studies have provided insights into the antitumor

activities of AKT inhibitors [65,66]. The future in vitro and in vivo studies will be crucial to confirm the efficacy of these phytochemicals in inhibiting AKT2 and reducing tumor progression. Given that AKT signaling also intersects neurodegenerative pathways, these inhibitors could potentially be explored for neuroprotective applications as well.

5. Conclusion

The AKT2 isoform plays a pivotal role in cancer progression, particularly in cancers such as breast, ovarian, and pancreatic. Targeting AKT2 for therapeutic interventions remains a significant focus due to its involvement in cell survival, proliferation, and glucose metabolism. This study identified phytochemicals, including millettone, uzarigenin, and dihydrobiochanin A, as potential inhibitors of AKT2. These compounds demonstrated higher binding affinities compared to the control AKT2 inhibitor ipatasertib, indicating their inhibitory potential. Molecular docking and molecular dynamics simulations validated the stability of these inhibitors in binding to AKT2, with uzarigenin showing superior stability and compact binding. This stability, coupled with the inhibition of key residues in the AKT2 active site, suggests that these compounds may offer new avenues for therapeutic development in cancer. Moreover, their effectiveness in targeting AKT2 suggests their applicability across multiple cancer types where AKT2 overexpression or dysregulation is a key driver of disease progression. These findings provide a strong foundation for the translational development of these inhibitors as targeted cancer therapies. Future in vitro and in vivo studies will be critical to confirm these findings, optimize their efficacy, and explore their potential clinical applications in diverse cancer contexts.

CRediT authorship contribution statement

Jibon Kumar Paul: Writing – original draft, Methodology, Investigation, Formal analysis, Data curation. **Mahir Azmal:** Writing – original draft, Methodology, Investigation, Formal analysis, Data curation. **Md Naimul Haque Shohan:** Investigation, Data curation. **Mohua Mrinmoy:** Methodology, Data curation. **ANM Shah Newaz Been Haque:** Methodology, Data curation. **Omar Faruk Talukder:** Methodology, Data curation. **Ajit Ghosh:** Writing – review & editing, Supervision, Resources, Project administration, Funding acquisition, Conceptualization.

Submission declaration and verification

The work presented is not being considered for publication elsewhere, and all authors have approved its submission. If accepted, it will not be published in the same form, either in English or any other language, including electronic formats, without prior written permission from the copyright holder.

Ethics declarations

Not applicable.

Data availability

For Phytochemical Search: Dr. Duke's Phytochemical and Ethnobotanical Databases.
For Phytochemical Downloads: PubChem Database.
For Protein: RCSB PDB database (2JDO)
Decoy analysis: DUD.E database.
Pathway analysis: KEGG: Kyoto Encyclopedia of Genes and Genomes - GenomeNet

Funding

The authors declare that no funds, grants, or other support were received during the preparation of this manuscript.

Declaration of competing interest

The authors declare that they have no known competing financial interests or personal relationships that could have appeared to influence the work reported in this paper.

Acknowledgment

The authors acknowledge the logistic support and laboratory facilities of the Department of Biochemistry and Molecular Biology, Shahjalal University of Science and Technology, Sylhet, Bangladesh.

Appendix A. Supplementary data

Supplementary data to this article can be found online at https://doi.org/10.1016/j.heliyon.2025.e41897.

References

[1] Y. He, M.M. Sun, G.G. Zhang, J. Yang, K.S. Chen, W.W. Xu, B. Li, Targeting PI3K/Akt signal transduction for cancer therapy, Signal Transduct Target Ther 6 (2021) 425, https://doi.org/10.1038/s41392-021-00828-5.

[2] A. Glaviano, A.S.C. Foo, H.Y. Lam, K.C.H. Yap, W. Jacot, R.H. Jones, H. Eng, M.G. Nair, P. Makvandi, B. Geoerger, M.H. Kulke, R.D. Baird, J.S. Prabhu, D. Carbone, C. Pecoraro, D.B.L. Teh, G. Sethi, V. Cavalieri, K.H. Lin, N.R. Javidi-Sharifi, E. Toska, M.S. Davids, J.R. Brown, P. Diana, J. Stebbing, D.A. Fruman, A. P. Kumar, PI3K/AKT/mTOR signaling transduction pathway and targeted therapies in cancer, Mol. Cancer 22 (2023) 138, https://doi.org/10.1186/s12943-023-01827-6.

[3] B.D. Manning, A. Toker, AKT/PKB signaling: navigating the network, Cell 169 (2017) 381–405, https://doi.org/10.1016/j.cell.2017.04.001.

[4] N. Chalhoub, S.J. Baker, PTEN and the PI3-kinase pathway in cancer, Annu. Rev. Pathol. 4 (2009) 127–150, https://doi.org/10.1146/annurev.pathol.4.110807.092311.

[5] C. Dong, J. Wu, Y. Chen, J. Nie, C. Chen, Activation of PI3K/AKT/mTOR pathway causes drug resistance in breast cancer, Front. Pharmacol. 12 (2021) 628690, https://doi.org/10.3389/fphar.2021.628690.

[6] X. Shi, X. Wang, W. Yao, D. Shi, X. Shao, Z. Lu, Y. Chai, J. Song, W. Tang, X. Wang, Mechanism insights and therapeutic intervention of tumor metastasis: latest developments and perspectives, Sig Transduct Target Ther 9 (2024) 1–46, https://doi.org/10.1038/s41392-024-01885-2.

[7] G.M. Nitulescu, D. Margina, P. Juzenas, Q. Peng, O.T. Olaru, E. Saloustros, C. Fenga, D.A. Spandidos, M. Libra, A.M. Tsatsakis, Akt inhibitors in cancer treatment: the long journey from drug discovery to clinical use, Int. J. Oncol. 48 (2015) 869–885, https://doi.org/10.3892/ijo.2015.3306. Review).

[8] S. Koseoglu, Z. Lu, C. Kumar, P. Kirschmeier, J. Zou, AKT1, AKT2 and AKT3-dependent cell survival is cell line-specific and knockdown of all three isoforms selectively induces apoptosis in 20 human tumor cell lines, Cancer Biol. Ther. 6 (2007) 755–762, https://doi.org/10.4161/cbt.6.5.3995.

[9] Y. Peng, Y. Wang, C. Zhou, W. Mei, C. Zeng, PI3K/Akt/mTOR pathway and its role in cancer therapeutics: are we making headway? Front. Oncol. 12 (2022) 819128 https://doi.org/10.3389/fonc.2022.819128.

[10] J. LoPiccolo, G.M. Blumenthal, W.B. Bernstein, P.A. Dennis, Targeting the PI3K/Akt/mTOR pathway: effective combinations and clinical considerations, Drug Resist Updat 11 (2008) 32–50, https://doi.org/10.1016/j.drup.2007.11.003.

[11] N. Coleman, J.T. Moyers, A. Harbery, I. Vivanco, T.A. Yap, Clinical development of AKT inhibitors and associated predictive biomarkers to guide patient treatment in cancer medicine, Pharmacogenomics Personalized Med. 14 (2021) 1517, https://doi.org/10.2147/PGPM.S305068.

[12] H. Hirai, H. Sootome, Y. Nakatsuru, K. Miyama, S. Taguchi, K. Tsujioka, Y. Ueno, H. Hatch, P.K. Majumder, B.-S. Pan, H. Kotani, MK-2206, an allosteric Akt inhibitor, enhances antitumor efficacy by standard chemotherapeutic agents or molecular targeted drugs in vitro and in vivo, Mol. Cancer Therapeut. 9 (2010) 1956–1967, https://doi.org/10.1158/1535-7163.MCT-09-1012.

[13] H.-L. Gao, Q. Cui, J.-Q. Wang, C.R. Ashby, Y. Chen, Z.-X. Shen, Z.-S. Chen, The AKT inhibitor, MK-2206, attenuates ABCG2-mediated drug resistance in lung and colon cancer cells, Front. Pharmacol. 14 (2023), https://doi.org/10.3389/fphar.2023.1235285.

[14] M. Wylaź, A. Kaczmarska, D. Pajor, M. Hryniewicki, D. Gil, J. Dulińska-Litewka, Exploring the role of PI3K/AKT/mTOR inhibitors in hormone-related cancers: a focus on breast and prostate cancer, Biomed. Pharmacother. 168 (2023) 115676, https://doi.org/10.1016/j.biopha.2023.115676.

[15] N. Coleman, J.T. Moyers, A. Harbery, I. Vivanco, T.A. Yap, Clinical development of AKT inhibitors and associated predictive biomarkers to guide patient treatment in cancer medicine, Pharmgenomics Pers Med 14 (2021) 1517–1535, https://doi.org/10.2147/PGPM.S305068.

[16] Y.-Y. Wu, H.-C. Wu, J.-E. Wu, K.-Y. Huang, S.-C. Yang, S.-X. Chen, C.-J. Tsao, K.-F. Hsu, Y.-L. Chen, T.-M. Hong, The dual PI3K/mTOR inhibitor BEZ235 restricts the growth of lung cancer tumors regardless of EGFR status, as a potent accompanist in combined therapeutic regimens, J. Exp. Clin. Cancer Res. 38 (2019) 282, https://doi.org/10.1186/s13046-019-1282-0.

[17] P. Garg, J. Malhotra, P. Kulkarni, D. Horne, R. Salgia, S.S. Singhal, Emerging therapeutic strategies to overcome drug resistance in cancer cells, Cancers 16 (2024) 2478, https://doi.org/10.3390/cancers16132478.

[18] I. Bansal, A.K. Pandey, M. Ruwali, Small-molecule inhibitors of kinases in breast cancer therapy: recent advances, opportunities, and challenges, Front. Pharmacol. 14 (2023) 1244597, https://doi.org/10.3389/fphar.2023.1244597.

[19] J.K. Paul, M. Azmal, A.S.N.B. Haque, O.F. Talukder, M. Meem, A. Ghosh, Phytochemical-mediated modulation of signaling pathways: a promising avenue for drug discovery, Advances in Redox Research 13 (2024) 100113, https://doi.org/10.1016/j.arres.2024.100113.

[20] S. Vitale, S. Colanero, M. Placidi, G. Di Emidio, C. Tatone, F. Amicarelli, A.M. D'Alessandro, Phytochemistry and biological activity of medicinal plants in wound healing: an Overview of current research, Molecules 27 (2022) 3566, https://doi.org/10.3390/molecules27113566.

[21] M. Sohel, S. Aktar, P. Biswas, MdA. Amin, MdA. Hossain, N. Ahmed, MdI.H. Mim, F. Islam, A.A. Mamun, Exploring the anti-cancer potential of dietary phytochemicals for the patients with breast cancer: a comprehensive review, Cancer Med. 12 (2023) 14556–14583, https://doi.org/10.1002/cam4.5984.

[22] P.C. Situmorang, S. Ilyas, S.E. Nugraha, R.A. Syahputra, N.M.A. Nik Abd Rahman, Prospects of compounds of herbal plants as anticancer agents: a comprehensive review from molecular pathways, Front. Pharmacol. 15 (2024), https://doi.org/10.3389/fphar.2024.1387866.

[23] MdA. Rahman, MdA. Hannan, R. Dash, M.D.H. Rahman, R. Islam, M.J. Uddin, A.A.M. Sohag, MdH. Rahman, H. Rhim, Phytochemicals as a complement to cancer chemotherapy: pharmacological modulation of the autophagy-apoptosis pathway, Front. Pharmacol. 12 (2021) 639628, https://doi.org/10.3389/fphar.2021.639628.

[24] J.K. Paul, M. Azmal, A.S.N.B. Haque, O.F. Talukder, M. Meem, A. Ghosh, Phytochemical-mediated modulation of signaling pathways: a promising avenue for drug discovery, Advances in Redox Research 13 (2024) 100113, https://doi.org/10.1016/j.arres.2024.100113.

[25] J. Israr, M.A. Khan, S. Misra, D. Gupta, N. Singh, R. Ahmad, S. Siddiqui, In silico screening and in vitro cytotoxicity study of Achyranthes aspera phytochemicals against oral cancer: a possible step towards the development of anti-cancer agents. http://Www.Eurekaselect.Com. (Accessed 29 December 2024). https://www.eurekaselect.com/article/141646.

[26] C.P. Ong, W.L. Lee, Y.Q. Tang, W.H. Yap, Honokiol: a review of its anticancer potential and mechanisms, Cancers 12 (2019) 48, https://doi.org/10.3390/cancers12010048.

[27] M.M. Saleh, Z.E. Darwish, M.I. El Nouaem, N.A. Fayed, G.M. Mourad, O.R. Ramadan, The potential preventive effect of dietary phytochemicals in Vivo, BDJ Open 9 (2023) 1–10, https://doi.org/10.1038/s41405-023-00157-5.

[28] M.B. Ahmed, S.U. Islam, A.A.A. Alghamdi, M. Kamran, H. Ahsan, Y.S. Lee, Phytochemicals as chemo-preventive agents and signaling molecule modulators: current role in cancer therapeutics and inflammation, Int. J. Mol. Sci. 23 (2022) 15765, https://doi.org/10.3390/ijms232415765.

[29] V. von Manstein, C.M. Yang, D. Richter, N. Delis, V. Vafaizadeh, B. Groner, Resistance of cancer cells to targeted therapies through the activation of compensating signaling loops, Curr. Signal Transduct. Ther. 8 (2013) 193–202, https://doi.org/10.2174/15743624096661402062219 31.

[30] M. Farhan, A. Rizvi, M. Aatif, A. Ahmad, Current understanding of flavonoids in cancer therapy and prevention, Metabolites 13 (2023) 481, https://doi.org/10.3390/metabo13040481.

[31] T.G. Davies, M.L. Verdonk, B. Graham, S. Saalau-Bethell, C.C.F. Hamlett, T. McHardy, I. Collins, M.D. Garrett, P. Workman, S.J. Woodhead, H. Jhoti, D. Barford, A structural comparison of inhibitor binding to PKB, PKA and PKA-PKB chimera, J. Mol. Biol. 367 (2007) 882–894, https://doi.org/10.1016/j.jmb.2007.01.004.

[32] W. Tian, C. Chen, X. Lei, J. Zhao, J. Liang, CASTp 3.0: computed atlas of surface topography of proteins, Nucleic Acids Res. 46 (2018) W363–W367, https://doi.org/10.1093/nar/gky473.

[33] D.E.V. Pires, T.L. Blundell, D.B. Ascher, pkCSM: predicting small-molecule pharmacokinetic and toxicity properties using graph-based signatures, J. Med. Chem. 58 (2015) 4066–4072, https://doi.org/10.1021/acs.jmedchem.5b00104.

[34] A. Daina, O. Michielin, V. Zoete, SwissADME: a free web tool to evaluate pharmacokinetics, drug-likeness and medicinal chemistry friendliness of small molecules, Sci. Rep. 7 (2017) 42717, https://doi.org/10.1038/srep42717.

[35] S. Dallakyan, A.J. Olson, Small-molecule library screening by docking with PyRx, Methods Mol. Biol. 1263 (2015) 243–250, https://doi.org/10.1007/978-1-4939-2269-7_19.

[36] M.M. Mysinger, M. Carchia, JohnJ. Irwin, B.K. Shoichet, Directory of useful decoys, enhanced (DUD-E): better ligands and decoys for better benchmarking, J. Med. Chem. 55 (2012) 6582–6594, https://doi.org/10.1021/jm300687e.

[37] N.M. O'Boyle, M. Banck, C.A. James, C. Morley, T. Vandermeersch, G.R. Hutchison, Open Babel: an open chemical toolbox, J. Cheminf. 3 (2011) 33, https://doi.org/10.1186/1758-2946-3-33.
[38] B. Toson, I.S. Fortes, R. Roesler, S.F. Andrade, Targeting Akt/PKB in pediatric tumors: a review from preclinical to clinical trials, Pharmacol. Res. 183 (2022) 106403, https://doi.org/10.1016/j.phrs.2022.106403.
[39] Z. Zhao, L. Xie, P.E. Bourne, Structural insights into characterizing binding sites in EGFR kinase mutants, J. Chem. Inf. Model. 59 (2019) 453–462, https://doi.org/10.1021/acs.jcim.8b00458.
[40] I. Bártová, M. Otyepka, Z. Kříž, J. Koča, Activation and inhibition of cyclin-dependent kinase-2 by phosphorylation; a molecular dynamics study reveals the functional importance of the glycine-rich loop, Protein Sci. 13 (2004) 1449–1457, https://doi.org/10.1110/ps.03578504.
[41] B. Chandrasekaran, S.N. Abed, O. Al-Attraqchi, K. Kuche, R.K. Tekade, Chapter 21 - computer-aided prediction of pharmacokinetic (ADMET) properties, in: R. K. Tekade (Ed.), Dosage Form Design Parameters, Academic Press, 2018, pp. 731–755, https://doi.org/10.1016/B978-0-12-814421-3.00021-X.
[42] J. Limantoro, B.G. de Liyis, J.C. Sutedja, Akt signaling pathway: a potential therapy for Alzheimer's disease through glycogen synthase kinase 3 beta inhibition, the Egyptian Journal of Neurology, Psychiatry and Neurosurgery 59 (2023) 147, https://doi.org/10.1186/s41983-023-00751-2.
[43] F. Martorana, G. Motta, G. Pavone, L. Motta, S. Stella, S.R. Vitale, L. Manzella, P. Vigneri, AKT inhibitors: new weapons in the fight against breast cancer? Front. Pharmacol. 12 (2021) https://doi.org/10.3389/fphar.2021.662232.
[44] E. Gonzalez, T.E. McGraw, The Akt kinases: isoform specificity in metabolism and cancer, Cell Cycle 8 (2009) 2502–2508, https://doi.org/10.4161/cc.8.16.9335.
[45] E. Tortorella, S. Giantulli, A. Sciarra, I. Silvestri, AR and PI3K/AKT in prostate cancer: a tale of two interconnected pathways, Int. J. Mol. Sci. 24 (2023) 2046, https://doi.org/10.3390/ijms24032046.
[46] A. Naeem, P. Hu, M. Yang, J. Zhang, Y. Liu, W. Zhu, Q. Zheng, Natural products as anticancer agents: current status and future perspectives, Molecules 27 (2022) 8367, https://doi.org/10.3390/molecules27238367.
[47] M.S. Hossan, Z.-Y. Chan, H.M. Collins, F.N. Shipton, M.S. Butler, M. Rahmatullah, J.B. Lee, P. Gershkovich, L. Kagan, T.-J. Khoo, C. Wiart, T.D. Bradshaw, Cardiac glycoside cerberin exerts anticancer activity through PI3K/AKT/mTOR signal transduction inhibition, Cancer Lett. 453 (2019) 57–73, https://doi.org/10.1016/j.canlet.2019.03.034.
[48] D. Reddy, R. Kumavath, P. Ghosh, D. Barh, Lanatoside C induces G2/M cell cycle arrest and suppresses cancer cell growth by attenuating MAPK, Wnt, JAK-STAT, and PI3K/AKT/mTOR signaling pathways, Biomolecules 9 (2019) 792, https://doi.org/10.3390/biom9120792.
[49] Z. Davoodi-Moghaddam, F. Jafari-Raddani, M. Delshad, A. Pourbagheri-Sigaroodi, D. Bashash, Inhibitors of the PI3K/AKT/mTOR pathway in human malignancies; trend of current clinical trials, J. Cancer Res. Clin. Oncol. 149 (2023) 15293–15310, https://doi.org/10.1007/s00432-023-05277-x.
[50] S. Pothongsrisit Iksen, V. Pongrakhananon, Targeting the PI3K/AKT/mTOR signaling pathway in lung cancer: an update regarding potential drugs and natural products, Molecules 26 (2021) 4100, https://doi.org/10.3390/molecules26134100.
[51] Y. Chen, W. Guan, M.-L. Wang, X.-Y. Lin, PI3K-AKT/mTOR signaling in psychiatric disorders: a valuable target to stimulate or suppress? Int. J. Neuropsychopharmacol. 27 (2024) pyae010 https://doi.org/10.1093/ijnp/pyae010.
[52] R. Liu, Y. Chen, G. Liu, C. Li, Y. Song, Z. Cao, W. Li, J. Hu, C. Lu, Y. Liu, PI3K/AKT pathway as a key link modulates the multidrug resistance of cancers, Cell Death Dis. 11 (2020) 1–12, https://doi.org/10.1038/s41419-020-02998-6.
[53] A. Glaviano, A.S.C. Foo, H.Y. Lam, K.C.H. Yap, W. Jacot, R.H. Jones, H. Eng, M.G. Nair, P. Makvandi, B. Geoerger, M.H. Kulke, R.D. Baird, J.S. Prabhu, D. Carbone, C. Pecoraro, D.B.L. Teh, G. Sethi, V. Cavalieri, K.H. Lin, N.R. Javidi-Sharifi, E. Toska, M.S. Davids, J.R. Brown, P. Diana, J. Stebbing, D.A. Fruman, A. P. Kumar, PI3K/AKT/mTOR signaling transduction pathway and targeted therapies in cancer, Mol. Cancer 22 (2023) 138, https://doi.org/10.1186/s12943-023-01827-6.
[54] F. Fontana, G. Giannitti, S. Marchesi, P. Limonta, The PI3K/Akt pathway and glucose metabolism: a dangerous liaison in cancer, Int. J. Biol. Sci. 20 (2024) 3113–3125, https://doi.org/10.7150/ijbs.89942.
[55] X. Xie, R. Shu, C. Yu, Z. Fu, Z. Li, Mammalian AKT, the emerging roles on mitochondrial function in diseases, Aging and Disease 13 (2022) 157–174, https://doi.org/10.14336/AD.2021.0729.
[56] MdK.H. Arnab, MdR. Islam, M.S. Rahman, A comprehensive review on phytochemicals in the treatment and prevention of pancreatic cancer: focusing on their mechanism of action, Health Sci Rep 7 (2024) e2085, https://doi.org/10.1002/hsr2.2085.
[57] I. Vivanco, C.L. Sawyers, The phosphatidylinositol 3-Kinase–AKT pathway in human cancer, Nat. Rev. Cancer 2 (2002) 489–501, https://doi.org/10.1038/nrc839.
[58] H.-W. Cheng, Y.-F. Chen, J.-M. Wong, C.-W. Weng, H.-Y. Chen, S.-L. Yu, H.-W. Chen, A. Yuan, J.J.W. Chen, Cancer cells increase endothelial cell tube formation and survival by activating the PI3K/Akt signalling pathway, J. Exp. Clin. Cancer Res. 36 (2017) 27, https://doi.org/10.1186/s13046-017-0495-3.
[59] D.A. Altomare, J.R. Testa, Perturbations of the AKT signaling pathway in human cancer, Oncogene 24 (2005) 7455–7464, https://doi.org/10.1038/sj.onc.1209085.
[60] S. Noorolyai, N. Shajari, E. Baghbani, S. Sadreddini, B. Baradaran, The relation between PI3K/AKT signalling pathway and cancer, Gene 698 (2019) 120–128, https://doi.org/10.1016/j.gene.2019.02.076.
[61] F. Rascio, F. Spadaccino, M.T. Rocchetti, G. Castellano, G. Stallone, G.S. Netti, E. Ranieri, The pathogenic role of PI3K/AKT pathway in cancer onset and drug resistance: an updated review, Cancers 13 (2021) 3949, https://doi.org/10.3390/cancers13163949.
[62] Y. Cheng, Y. Zhang, L. Zhang, X. Ren, K.J. Huber-Keener, X. Liu, L. Zhou, J. Liao, H. Keihack, L. Yan, E. Rubin, J.-M. Yang, MK-2206, a novel allosteric inhibitor of Akt, synergizes with gefitinib against malignant glioma via modulating both autophagy and apoptosis, Mol. Cancer Therapeut. 11 (2012) 154–164, https://doi.org/10.1158/1535-7163.MCT-11-0606.
[63] H. Yadav, A. Mahalvar, M. Pradhan, K. Yadav, K. Kumar Sahu, R. Yadav, Exploring the potential of phytochemicals and nanomaterial: a boon to antimicrobial treatment, Medicine in Drug Discovery 17 (2023) 100151, https://doi.org/10.1016/j.medidd.2023.100151.
[64] Z. Lei, Q. Tian, Q. Teng, J.N.D. Wurpel, L. Zeng, Y. Pan, Z. Chen, Understanding and targeting resistance mechanisms in cancer, MedComm (2020) 4 (2023) e265, https://doi.org/10.1002/mco2.265.
[65] Y. Luo, A.R. Shoemaker, X. Liu, K.W. Woods, S.A. Thomas, R. de Jong, E.K. Han, T. Li, V.S. Stoll, J.A. Powlas, A. Oleksijew, M.J. Mitten, Y. Shi, R. Guan, T. P. McGonigal, V. Klinghofer, E.F. Johnson, J.D. Leverson, J.J. Bouska, M. Mamo, R.A. Smith, E.E. Gramling-Evans, B.A. Zinker, A.K. Mika, P.T. Nguyen, T. Oltersdorf, S.H. Rosenberg, Q. Li, V.L. Giranda, Potent and selective inhibitors of Akt kinases slow the progress of tumors in vivo, Mol. Cancer Therapeut. 4 (2005) 977–986, https://doi.org/10.1158/1535-7163.MCT-05-0005.
[66] M. Dumble, M.-C. Crouthamel, S.-Y. Zhang, M. Schaber, D. Levy, K. Robell, Q. Liu, D.J. Figueroa, E.A. Minthorn, M.A. Seefeld, M.B. Rouse, S.K. Rabindran, D. A. Heerding, R. Kumar, Discovery of novel AKT inhibitors with enhanced anti-tumor effects in combination with the MEK inhibitor, PLoS One 9 (2014) e100880, https://doi.org/10.1371/journal.pone.0100880.